Translational Oncology 40 (2024) 101875

Contents lists available at ScienceDirect

Translational Oncology

journal homepage: www.elsevier.com/locate/tranon

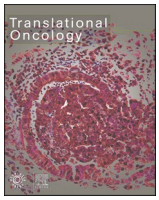

Original Research

Elucidating cellular response to treatment with viral immunotherapies in pediatric high-grade glioma and medulloblastoma

Eric M. Thompson [a,b,*], Kyung-Don Kang [c,d], Kevin Stevenson [e], Hengshan Zhang [b], Matthias Gromeier [b], David Ashley [b], Michael Brown [b], Gregory K. Friedman [c,d]

[a] Department of Neurosurgery, University of Chicago, Chicago, IL, USA
[b] Department of Neurosurgery, Duke University, Durham, NC, USA
[c] Department of Pediatrics, University of Alabama at Birmingham, Birmingham, AL, USA
[d] The University of Texas MD Anderson Cancer Center, Houston, TX, USA
[e] Department of Biostatistics and Bioinformatics, Duke University School of Medicine, Durham, NC, USA

ARTICLE INFO

Keywords:
PVSRIPO
G207
Oncolytic virus
Viral immunotherapy
Medulloblastoma
Pediatric high-grade glioma
Cell response
RNA sequencing

ABSTRACT

HSV G207, a double-stranded, DNA virus, and the polio:rhinovirus chimera, PVSRIPO, a single positive-strand RNA virus, are viral immunotherapies being used to treat pediatric malignant brain tumors in clinical trials. The purpose of this work is to elucidate general response patterns and putative biomarkers of response. Multiple pediatric high-grade glioma and medulloblastoma cell lines were treated with various multiplicities of infection of G207 or PVSRIPO. There was a significant inverse correlation between expression of one HSV cellular receptor, CD111, and the lethal dose of 50% of cells (LD50) of cells treated with G207 ($r = -0.985$, $P<0.001$) but no correlation between PVSRIPO cellular receptor expression (CD155) and LD50. RNA sequencing of control cells and cells treated for 8 and 24 h revealed that there were few shared differentially expressed (DE) genes between cells treated with PVSRIPO and G207: *GCLM*, *LANCL2*, and *RBM3* were enriched whilst *ADAMTS1* and *VEGFA* were depleted. Likewise, there were few shared DE genes enriched between medulloblastoma and high-grade glioma cell lines treated with G207: *GPSM2, CHECK2, SEPTIN2, EIF4G2, GCLM, GDAP1, LANCL2,* and *PWP1*. Treatment with G207 and PVSRIPO appear to cause disparate gene enrichment and depletion suggesting disparate molecular mechanisms in malignant pediatric brain tumors.

Introduction

Two of the most common malignant brain tumors in children are medulloblastoma and pediatric high-grade glioma (pHGG). Currently, treatment of these tumor consists of maximal safe resection typically followed by radiation and chemotherapy. However, this treatment strategy results in five-year overall survival (OS) ranging from 85% for average-risk disease to ~50% for high-risk disease [1,2] for medulloblastoma and a median overall survival of only 16 months in pHGG [3]. The prognosis for patients with recurrent medulloblastoma and pHGG is far worse.

Viral immunotherapy is a promising alternative to conventional radiation and chemotherapy to treat recurrent medulloblastoma and pHGG. Two viral immunotherapies currently in early-phase clinical trials for the treatment of recurrent medulloblastoma and pHGG include the recombinant polio:rhinovirus chimera, PVSRIPO (NCT03043391) [4] and genetically engineered herpes simplex virus (HSV), G207 (NCT02457845 and NCT03911388) [4–6]. Additionally, PVSRIPO has been explored in adults with recurrent glioblastoma in Phase I (NCT01491893) [5] and Phase II trials (NCT02986178), while G207 has been explored in three Phase I trials alone and in combination with radiation therapy (NCT00157703) [7–9]. These studies demonstrated encouraging OS for some patients [5], however, responses have been variable, and it is unknown why some patients have excellent responses to viral immunotherapy while others do not. The molecular mechanisms governing antitumor effects of these viral immunotherapies are unclear.

We sought to explore the molecular pathways and genes elicited by PVSRIPO and G207 infection of glioma and medulloblastoma models. Using cell viability assays, flow cytometry, and RNA sequencing, we found that the two viral immunotherapies had few molecular

Abbreviations: pHGG, pediatric high-grade glioma; OS, overall survival.

* Corresponding author at: The University of Chicago, 5841 S. Maryland Ave, MC 3026, Chicago, IL 60637, USA.
E-mail address: eric.thompson@uchicago.edu (E.M. Thompson).

https://doi.org/10.1016/j.tranon.2024.101875
Received 19 July 2023; Received in revised form 8 December 2023; Accepted 27 December 2023
Available online 5 January 2024

similarities and many dissimilarities in terms of cell death, cellular viral receptor number, and cellular response to viral infection. These results imply non-overlapping mechanisms of action and sensitivities between these clinically relevant viral immunotherapy strategies.

Materials and methods

Human derived medulloblastoma and high-grade glioma cells

The medulloblastoma cell lines D324 (DAOY), D341, and D556 were obtained from the lab of Darell Bigner at Duke University. D283 were obtained from the American Type Culture Collection (ATCC). 8A-Med was obtained from the lab of Marc Remke. The pHGG line D456 was obtained from the lab of Darell Bigner (Duke University), the glioblastoma cell line U87 was obtained from the lab of Michael Brown (Duke University) and the pHGG line X21584 was obtained from the lab of Gregory Friedman. All cells were cultured in DMEM-F12 + 10%FBS, 1% NEAA, and 1% glutamine except X21584 which was cultures in neurobasal medium plus FGF, EGF, B-27 supplement, L-glutamine, amphotericin B, and gentamicin, and D341 which was cultured in Improved MEM Zinc option.

All cell lines have been previously validated in the literature. The medulloblastoma cell lines DAOY [10], D283 [11,12], D341, D556, and 8A-Med have been extensively characterized [13–15]. DAOY may be in the SHH subgroup whereas the rest are likely Group 3 subgroup [15,16]. D456 was derived from a frontal lobe glioblastoma in an 8 year old female [17]. U87 is likely a glioblastoma from an unknown origin [18,19] while X21584 was derived from a high grade glioma of a 12 year male [20].

Viral infection of tumor cells

PVSRIPO and G207 were derived and propagated as previously described [20–22]. Briefly, PVSRIPO was grown in HeLa cells [23], purified using a 0.45 μm syringe filter, concentrated and filtered again through a 100 kDa filter (Millipore). G207 was grown in Vero cells and purified on OptiPrep™ gradients (AXIS-SHIELD Oslo, Norway) [24]. Titers were determined by plaque assay [23]. The effect of PVSRIPO and G207 medulloblastoma and glioblastoma cytotoxicity was determined using CellTiter-Glo, (Promega) per the manufacturer's protocol in triplicate. Briefly, 25,000 cells in 100 μL were plated (Greiner CELLSTAR®) 96 well plates, incubated for 8 h, then treated with either PVSRIPO or G207 at multiplicity of infection (MOI) 0, 0.01, 0.1, 1, 10, or 100 for 24 h (PVSRIPO) or 72 h (G207). Cell viability line graphs were created using GraphGad Prism 9 (La Jolla, CA).

RNA sequencing of medulloblastoma and pHGG cell lines

RNA sequencing was completed as previously described [25] for D283, D324, D341, and D556 medulloblastoma and D456 and X21584 pHGG for the following G207 treatment conditions: control (0 h), 8 h after viral infection, 24 h after viral infection. RNA sequencing was completed for D283, D324, D341, and D556 medulloblastoma for the following PVSRIPO treatment conditions: control (0 h), 8 h after viral infection, 24 h after viral infection. RNA sequencing for D456 and X21584 treated with PVSRIPO was not completed due to difficulties with cell viability/processing for sequencing. The Sequencing and Genomics Technologies (SGT) Core Facility at Duke University performed RNA-sequencing. Total RNA was extracted from cell pellets using the RNeasy Plus Mini Kit (Qiagen # 74,134). mRNA was enriched from total RNA and reversed transcribed into cDNA. Kapa mRNA HyperPrep Kit (Roche # KK8581) was used to build sequencing libraries. Libraries were pooled to equal number of moles and sequenced on the NovaSeq 6000 S2 flow cell to produce 50 base pair paired-end reads. Triplicates were run for all cell types and treatment conditions, each in two lanes.

Sample fastq files quality metrics were assessed via FastQC v0.11.9 and MultiQC v1.11. Next, the paired-end reads were aligned to the GRCh38.p14 human reference genome via STAR v2.7.2b with default parameter settings. Subsequently, post-alignment quality metrics were assessed via the log file output of STAR. Quantification and generation of the raw counts matrix was performed via featureCounts v1.6.3. Replicates were combined using the collapseReplicates function within DESeq2 R package v1.36.0. The raw counts matrix was then normalized and differential expression was calculated via DeSeq2 R package v1.36.0 with a design that combined the cell line and treatment metadata. The differentially expressed genes for each comparison were then ranked by log2FC and input into fgsea R package v1.23.4 for gene set enrichment analysis along with the Hallmark gene set collection from MSigDB. RStudio 2022.07.0 Build 548 running R version 4.2.1 was used for the analysis.

The R script is located in Supplementary Materials.

Unsupervised hierarchical clustering/heatmap using the geneset GOBP_DEFENSE_RESPONSE_TO_VIRUS (https://www.gsea-msigdb.org/gsea/msigdb/cards/GOBP_DEFENSE_RESPONSE_TO_VIRUS) was created using MORPHEUS (https://software.broadinstitute.org/morpheus/).

GraphPad Prism 9 was used to calculate Pearson r of virus LD50 and receptor number and paired t-test (two tailed) of resistant vs. sensitive number of genes. Volcano plots were created using VocaNoseR [26] in which Manhattan distance was used for ranking hits.

RNA sequencing and analysis of human specimens

For patient glioblastoma specimens, RNA-seq data of samples were aligned to GRCh38 using STAR (v2.4.0.1) and expression quantification per gene was computed by FeatureCounts (v1.4.6). The function "cpm" in R package EdgeR (v3.30.3) was used to normalize the raw counts into the counts per million (CPM). The batch effects were also removed during the normalization. Specimens were obtained from the clinical trial (NCT02986178), a Phase II trial of PVSRIPO for recurrent glioblastoma in adult patients. In clinical trials that treated pediatric patients with HGG with either PVSRIPO (NCT03043391) [4] or G207 (NCT02457845) [6], there was insufficient tissue to perform RNA sequencing.

Flow cytometry

To investigate expression of CD111 and CD155, neurospheres were dissociated into a single cell suspension using Accutase (Innovative Cell Technologies) or adherent cells were detached using Trypsin and prepared for fluorescence activated cell sorting (FACS) analysis. The following fluorochrome-conjugated monoclonal antibodies were used: PE anti-human CD111 (Nectin-1; BioLegend Cat# 340,404, RRID: AB_2,174,152) and APC anti-human CD155 (PVR; BioLegend Cat# 337,618, RRID:AB_2,565,815). Cells were analyzed with an Attune NxT Flow Cytometer (Thermo Fisher Scientific) in the UAB Flow Cytometry Core Facility, and the results were expressed as a percentage of gated cells for antibody binding using FlowJo software V10 (RRID: SCR_008520). Mean values from multiple determinations on separate dates and with separate cultures were calculated.

Results

pHGG and medulloblastoma demonstrate different sensitivities to G207 or PVSRIPO

To identify putative cellular mechanisms of resistance, we first sought to categorize medulloblastoma and pHGG cell lines as "sensitive" and "resistant" based on LD50 values after treatment with virotherapy and nonhierarchical clustering of RNA signatures. Cell viability assays were performed at standard time points (24 h for PVSRIPO and 72 h for G207) based on differences in viral replication rates. With PVSRIPO,

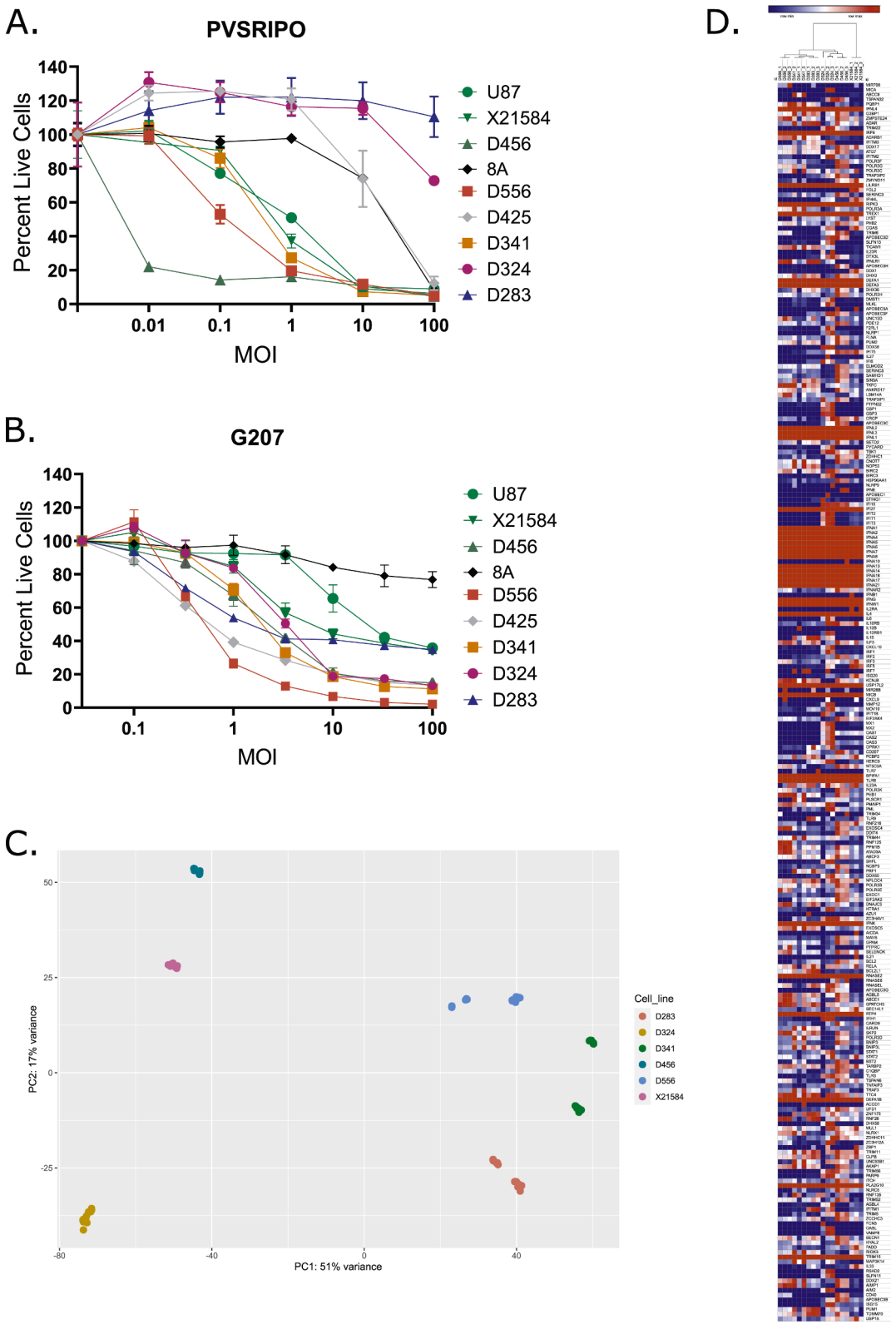

Fig. 1. Dose response curves of pHGG and medulloblastoma cell lines to viral immunotherapy. (A) Cell viability after treatment with PVSRIPO for 24 h. Note the separation of cell line viability at MOI 1; the cell lines D324, 8A, D425, D283 grouped together as more "resistant". (B) Cell viability after treatment of cells with G207 for 72 h. There was no clear grouping ("resistant" vs "sensitive") viability at MOI 1. (C) PCA plot of mRNA sequencing data of untreated medulloblastoma and pHGG cells demonstrates clustering of pHGG cells (D456, X21584). D324 or DAOY cells were distinct from other pHGG and medulloblastoma cells. (D) Unsupervised hierarchical clustering of D283, D324, D341, D556, D456, and X21584 cells using the geneset GOBP_DEFENSE_RESPONSE_TO_VIRUS, demonstrates grouping of D556/D341 cells and D283/D324 cells, similar to the grouping of the dose response curve at MOI 1 (A). MOI: multiplicity of infection.

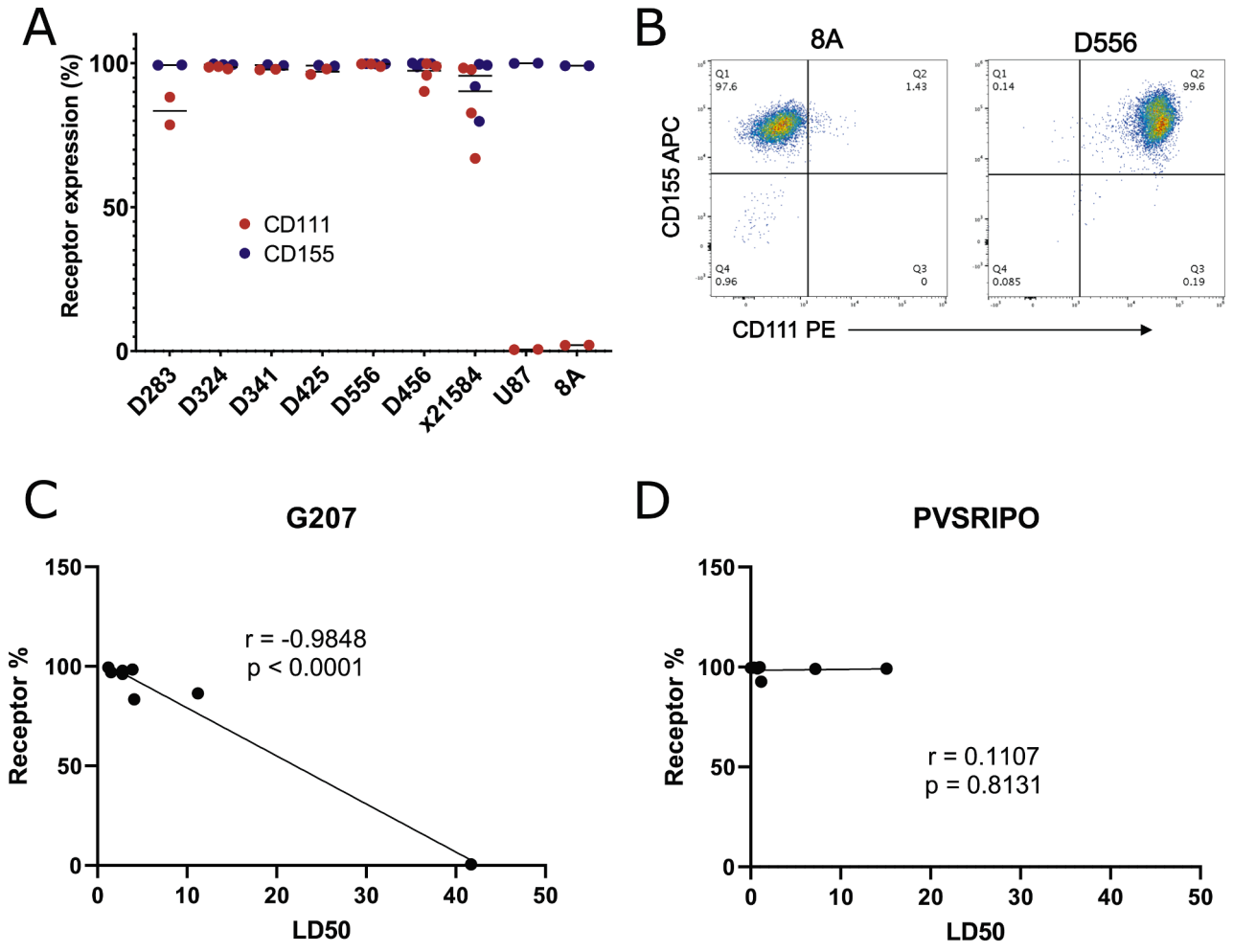

Fig. 2. Cell surface receptor expression is correlated with cytotoxicity for CD111 but not CD155. (A) Dot plot of Nectin-1 (CD111) receptor expression and Poliovirus receptor (CD155) expression by cell type as percentage of cells expressing receptor. (B) Scatter plot of flow cytometry data demonstrating Lack CD111 expression in 8A cells with robust CD155 expression vs. D556 cells demonstrating both robust CD111 and CD155 expression. (C) There is a significant inverse correlation between CD111 expression and LD50 from G207 treatment not seen in CD155 expression and LD50 from PVSRIPO treatment (D).

U87, X21584, D456, D341 and D556 had less than 50% viability at an MOI 1 (Fig. 1A). Based upon these results, D341 and D556 were categorized as "sensitive" to PVSRIPO while D283 and D324 were categorized as "resistant". These cells were thus selected to undergo RNA sequencing as described in Methods. With G207, there was a lack of a clear, natural separation of cell viability at MOI 1 (Fig. 1B); and therefore, this categorization scheme was not used for G207. D456 and X21584 were also selected for RNA sequencing as they are both pHGG cell lines.

Next, Principal Component Analysis (PCA) plot using RNA sequencing data of untreated cell types demonstrated relative clustering of the medulloblastoma cell lines D283, D341, and D556 while D324 and the pHGG cell lines D456 and X21584 had substantial variance (Fig. 1C). Nonhierarchical clustering of RNA sequencing using the geneset, GOBP_DEFENSE_RESPONSE_TO_VIRUS (http://www.gsea-msigdb.org/gsea/msigdb/cards/GOBP_DEFENSE_RESPONSE_TO_VIRUS), demonstrated adjacent clustering of cells in the following order: D556, D341, D283, D324, D456, X21584 (Fig. 1D).

Viral cellular entry molecule number correlates with cytotoxicity for G207 but not PVSRIPO

Previous work by our group demonstrated a significant inverse correlation between G207 sensitivity and expression of its cell surface receptor, nectin-1 (CD111) [20]. Flow cytometry was performed to quantify the expression of CD111 and CD155, the cell surface receptor for PVSRIPO [22]. Similar to previous findings, there was a strong inverse correlation between CD111 expression and LD50 to G207 ($r = -0.985$, $P < 0.001$, Fig. 2A). However, there was not a correlation between CD155 expression and LD50 to PVSRIPO ($r = 0.111$, $p = 0.813$, Fig. 2B) due to the near universal expression of CD155, and the exceedingly low number of CD155 moieties sufficient for virus entry [27], suggesting a different mechanism than receptor expression for decreased cytotoxicity of some cell lines to PVSRIPO. The flow cytometry gating strategy is located in Fig. S1.

pHGG and medulloblastoma response to virotherapy demonstrates enrichment and depletion in multiple cellular pathways and differentially expressed genes

Medulloblastoma and pHGG cells were not treated (controls) or treated for 8 h or 24 h with either G207 or PVSRIPO. Details of all significantly enriched and depleted hallmark pathways can be found in Tables S1 and S2, respectively. Graphical representation of the most significant hallmark pathways is located in Fig. 3. Notably, the hallmark pathways with the greatest number of enrichment, E2F targets, G2M checkpoints, mitotic spindle, and myc targets all fall into the hallmark process category "proliferation" with the first three representing cell cycle progression genesets [28].

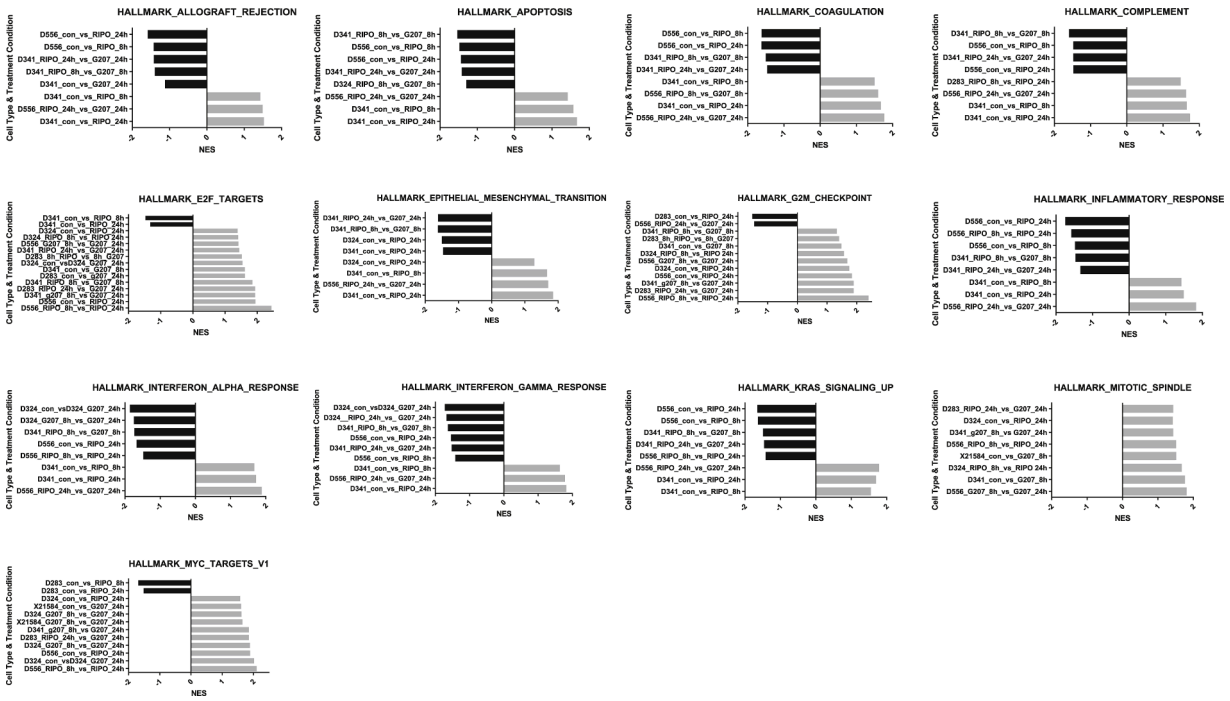

Fig. 3. The most common enriched and depleted hallmark pathways. Bar graphs of hallmark gene sets with at least eight significantly ($P \leq 0.05$) depleted (black) or enriched (gray) treatment comparisons. Treatment comparisons are on the y axis, NES on the x axis. NES: normalized enrichment score.

Table 1
Significantly Differentially Expressed Genes Enriched by G207 and PVSRIPO in Medulloblastoma.

Enriched	Control vs. 8 hrs	Control vs. 24 hrs	8 hrs vs. 24 hrs
	None	None	*GCLM* *LANCL2* *RBM3*
Depleted			
	ADAMTS1	*VEGFA*	None

Gene	Full name	Function	Reference
GCLM	glutamate-cysteine ligase modifier subunit	first rate limiting enzyme of glutathione synthesis	https://www.ncbi.nlm.nih.gov/gene/2730
LANCL2	LanC like glutathione S-transferase 2	involved in negative regulation of transcription	https://www.ncbi.nlm.nih.gov/gene/55915
RBM3	RNA binding motif protein 3	member of the glycine-rich RNA-binding protein family	https://www.ncbi.nlm.nih.gov/gene/5935
ADAMTS1	ADAM metallopeptidase with thrombospondin type 1 motif 1	Associated with inflammation	https://www.ncbi.nlm.nih.gov/gene/9510
VEGFA	vascular endothelial growth factor A	induces proliferation and migration of vascular endothelial cells, angiogenesis	https://www.ncbi.nlm.nih.gov/gene/7422

Medulloblastoma response to treatment with G207 and PVSRIPO differ

Details of significantly differentially expressed genes in all treatment groups can be found in Table S3. Despite the hundreds to thousands of differentially expressed genes for each treatment condition, there were only five DE genes shared by all medulloblastoma cell lines and G207 and PVSRIPO: *GCLM, LANCL2,* and *RBM3* were enriched while *ADAMTS1 and VEGFA* were depleted (Table 1). Treatment with PVSRIPO was associated with a larger number of DE genes compared to G207; control vs 8 h: 187 and 8, respectively; control vs 24 h: 146 and 26, respectively (Fig. 4A). PCA plots (Fig. 4B–D) visually demonstrate the clustering of cells treated with G207 vs. PVSRIPO while a volcano plot demonstrates the interaction effects between both time points (0, 8 h, 24 h) and treatment (G207 and PVSRIPO), controlling for both (Fig. 4E).

Medulloblastoma and pHGG cellular response to G207 infection

Multiple significantly enriched and depleted DE genes were shared by all medulloblastoma cell lines and pHGG cell lines (Table 2). Notably, both *GCLM* and *LANCL2* were enriched at 8- vs. 24-hour time points, two genes enriched after treatment with both PVSRIPO and G207 in medulloblastoma. Data for pHGG cellular response to PVSRIPO is not available due to cell viability/RNA processing difficulties.

Resistant vs. sensitive cellular response to PVSRIPO

Comparing untreated "resistant (D283, D324)" and "sensitive (D341, D556)" medulloblastoma cells, there were over 4000 significantly differentially expressed genes. The top 50 are highlighted in a volcano plot (Fig. 5A), demonstrating many more enriched signatures in the "sensitive cells". Treatment of "resistant" compared to "sensitive" medulloblastoma cell lines with PVSRIPO demonstrated a significantly lower number of resistant cell line depleted genes (Fig. 5B). Likewise,

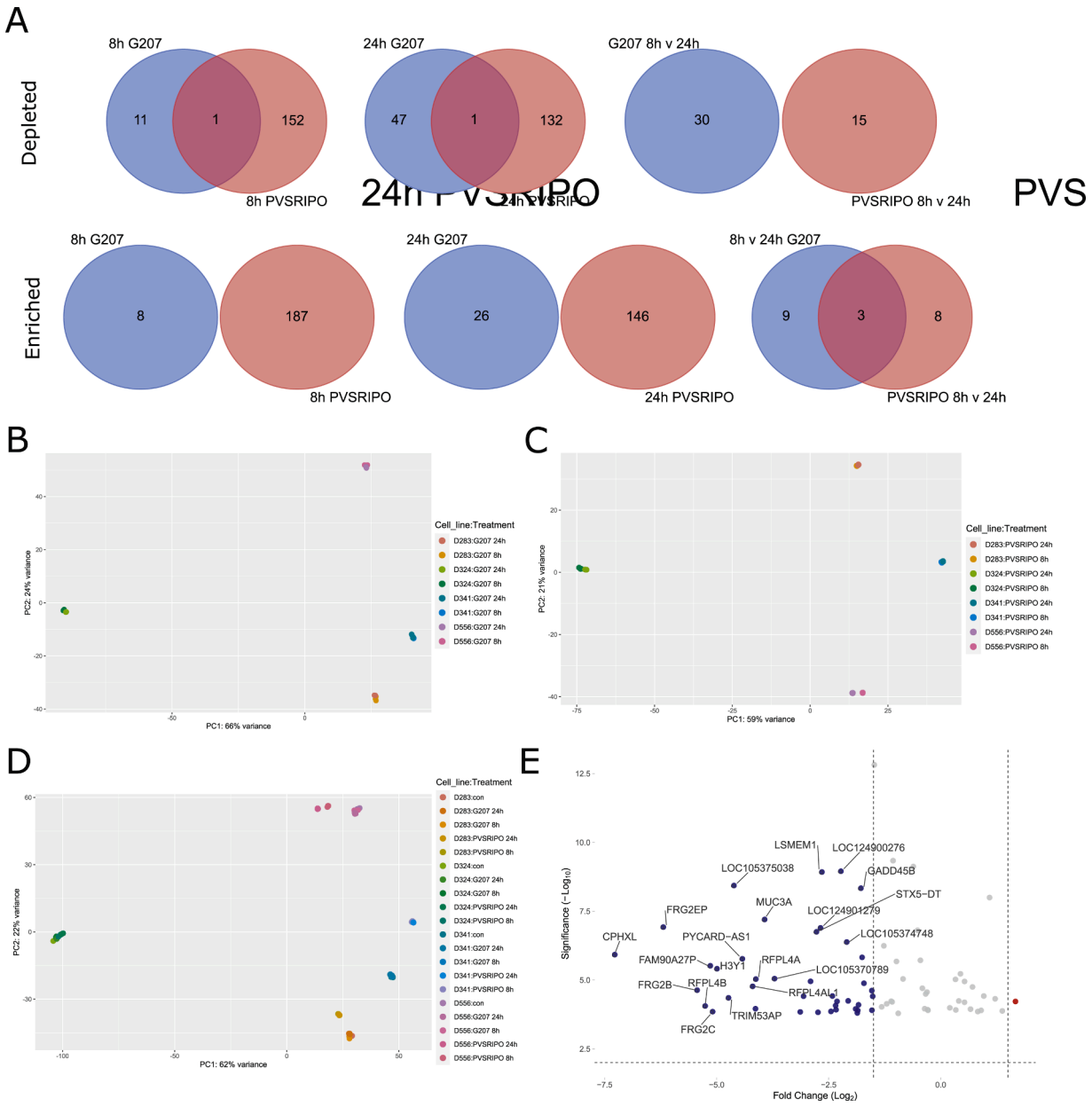

Fig. 4. Medulloblastoma cells response differently to treatment with G207 and PVSRIPO. (A) Venn diagram demonstrating minimal overlap in G207 and PVSRIPO of significantly differentially expressed genes. PCA plots of medulloblastoma cells treated with G207 (B), PVSRIPO (C), and the two graphs combined (D). (E) Volcano plot of differentially expressed genes of cells treated with PVSRIPO vs. G207 demonstrating the interaction effect between time point and treatment, controlling for both.

there was a decreased number of resistant cell line enriched genes (Fig. 5C), however, this difference did not achieve statistical significance.

Shared genes in poor survival in a clinical trial of glioblastoma and "resistant" medulloblastoma cell lines

We first analyzed RNA sequencing of patient recurrent glioblastoma samples taken prior to treatment with PVSRIPO in a Phase II clinical trial ("PVSRIPO in Recurrent Malignant Glioma", NCT02986178, https://www.clinicaltrials.gov/study/NCT02986178?term=pvsripo&page=1&rank=1). Patients were categorized by $<$ or $\geq$ one year OS after treatment with PVSRIPO. "Low" survival was defined as $<$ one year OS. The top 50 differentially expressed genes can be found in Table S4, Fig. 6. The only significantly different geneset in the comparison of these groups was the HALLMARK_EPITHELIAL_MESENCHYMAL_TRANSITION [29,30], adjusted $P<0.001$, NES 1.5949.

Next, we analyzed DE genes shared by both PVSRIPO "resistant" medulloblastoma and "low" survival in a Phase II trial of PVSRIPO for recurrent glioblastoma (NCT02986178) to determine the presence of any shared genes from each dataset. The following genes were enriched in both datasets: *CCDC13, LGR6, LMO2, LUM,* and *RARB* while the following genes were depleted in both datasets: *ADAMTS20, ANGPTL4, BEND, CSF1, FUT11, PCSK6, PLIN2,* and *PLS1* (Table 3). Notably, none of these genes were found in the "low" vs. "high" survival of the Phase II study indicating another putative set of biomarkers to predict response to PVSRIPO across tumor types.

Discussion

Both viral recombinants investigated in this study have the capacity to infect cancerous cells derived of malignant gliomas or

Table 2
Significantly differentially expressed genes in both medulloblastoma and HGG cell lines treated with G207.

	Gene	Gene function	Reference
Enriched			
Control vs. 8 hrs			
	GPSM2	cell surface G protein modulator	https://www.ncbi.nlm.nih.gov/gene/29899
	CHECK2	checkpoint regulator of cell cycle, possible tumor suppressor	https://www.ncbi.nlm.nih.gov/gene/11200
Control vs. 24 hrs			
	SEPTIN2	involved in identical protein binding including cilium, exocytosis, smoothened signaling	https://www.ncbi.nlm.nih.gov/gene/4735
8 hrs vs. 24 hrs			
	EIF4G2	involved in translation initiation	https://www.ncbi.nlm.nih.gov/gene/1982
	GCLM	first rate limiting enzyme of glutathione synthesis	https://www.ncbi.nlm.nih.gov/gene/2730
	GDAP1	member of ganglioside-induced differentiation family	https://www.ncbi.nlm.nih.gov/gene/54332
	LANCL2	involved in negative regulation of transcription	https://www.ncbi.nlm.nih.gov/gene/55915
	PWP1	largely unknown, cell cycle dependent	https://www.ncbi.nlm.nih.gov/gene/11137
Depleted			
Control vs. 8 hrs			
	LANCL2	involved in negative regulation of transcription	https://www.ncbi.nlm.nih.gov/gene/55915
	RASD1	member of Ras family of GTPases, induced by dexamethasone	https://www.ncbi.nlm.nih.gov/gene/51655
	RHOB	GTPase activity, involved in cell response to stress	https://www.ncbi.nlm.nih.gov/gene/388
Control vs. 24 hrs			
	ARC	involved in mRNA binding, cell migration, cytoskeleton organization	https://www.ncbi.nlm.nih.gov/gene/23237
	BCL2L11	BCL-2 family member, involved in apoptosis	https://www.ncbi.nlm.nih.gov/gene/10018
	CA2	isozyme of carbonic anhydrase	https://www.ncbi.nlm.nih.gov/gene/760
	CBX4	enables small ubiquitin-like modifier (SUMO) binding activity	https://www.ncbi.nlm.nih.gov/gene/8535
	CCDC137	enables RNA binding	https://www.ncbi.nlm.nih.gov/gene/339230
	CCN1	promotes cell adhesion	https://www.ncbi.nlm.nih.gov/gene/3491
	CCN2	involved in cell adhesion	https://www.ncbi.nlm.nih.gov/gene/1490
	EGR2	transcription factor	https://www.ncbi.nlm.nih.gov/gene/1959
	FRG2C	unknown, located in nucleus	https://www.ncbi.nlm.nih.gov/gene/100288801
	GADD45B	respond to cellular stress	https://www.ncbi.nlm.nih.gov/gene/4616
	JUNB	involved in transcription by RNA polymerase II	https://www.ncbi.nlm.nih.gov/gene/3726
	LOC124900276	"cuticle collagen 2-like", unknown	https://www.ncbi.nlm.nih.gov/gene/?term=LOC124900276
	MYLIP	interacts with myosin regulatory light chain	https://www.ncbi.nlm.nih.gov/gene/29116
	NFKBIA	member of NF-kappa-B inhibitor family	https://www.ncbi.nlm.nih.gov/gene/4792
	NXF1	member of nuclear RNA export factors	https://www.ncbi.nlm.nih.gov/gene/10482
	RASL11B	member of GTPase family similar to RAS	https://www.ncbi.nlm.nih.gov/gene/65997
	RGS2	GTPase activating protein	https://www.ncbi.nlm.nih.gov/gene/5997
	SGK1	kinase with role cellular stress response	https://www.ncbi.nlm.nih.gov/gene/6446
	ZNF296	enables DNA binding activity	https://www.ncbi.nlm.nih.gov/gene/162979
8 hrs vs. 24 hrs			
	CBX4	see above	
	CCN1	see above	
	JUNB	see above	
	LSMEM1	unknown, possible membrane component	https://www.ncbi.nlm.nih.gov/gene/286006
	MUC3A	epithelial glycoprotein, described in gastrointestinal cancer	https://www.ncbi.nlm.nih.gov/gene/4584#gene-expression
	NRARP	involved in Notch and Wnt signaling pathways	https://www.ncbi.nlm.nih.gov/gene/441478
	NXF1	see above	
	RASD1	see above	
	RSRP1	implicated in glioblastoma mesenchymal phenotype	PMID: 34,042,961
	ZNF296	see above	

medulloblastomas, by virtue of expression of polio- and HSV-1 entry receptors on such cellular hosts. However, the relative contributions of viral targeting of the neoplastic compartment to antitumor immunity likely differ considerably for both agents.

PVSRIPO primarily targets myeloid antigen presenting cells (dendritic cells/ macrophages) in patient *ex vivo* glioma slices [31] and in mouse glioma models [31]. Infection of the tumor myeloid infiltrate/CNS resident myeloid compartments—producing profound immune stimulation through endogenous, sustained type-I interferon release—is sufficient for generating tumor immune surveillance in mouse tumor models [21,31–33]. In contrast, immunotherapy mechanisms of oncolytic HSV-1 recombinants were shown to rely on cytopathogenic infection of neoplastic cells with a potential secondary role for myeloid bystanders [34].

In this work we analyzed the outcome of infection with either G207 or PVSRIPO in a panel of pHGG and medulloblastoma cell lines. We found a significant correlation between CD111 and lethality of cells treated with G207. This confirms our previous results in which a host of adult and pediatric HGG as well as embryonal tumors treated with G207 demonstrated a significant inverse correlation between CD111 and LD50 [20]. However, we did not find any correlation between CD155 expression and PVSRIPO lethality due to the universal high percentage of cells expressing CD155. Future research will determine if CD111 in tumor specimen will predict clinical outcomes in children with HGG and medulloblastoma.

A main objective of this study was to determine if there are common responses in infected cancerous cells to disparate viral immunotherapies, HSV G207, a double stranded DNA virus and the polio:rhinovirus

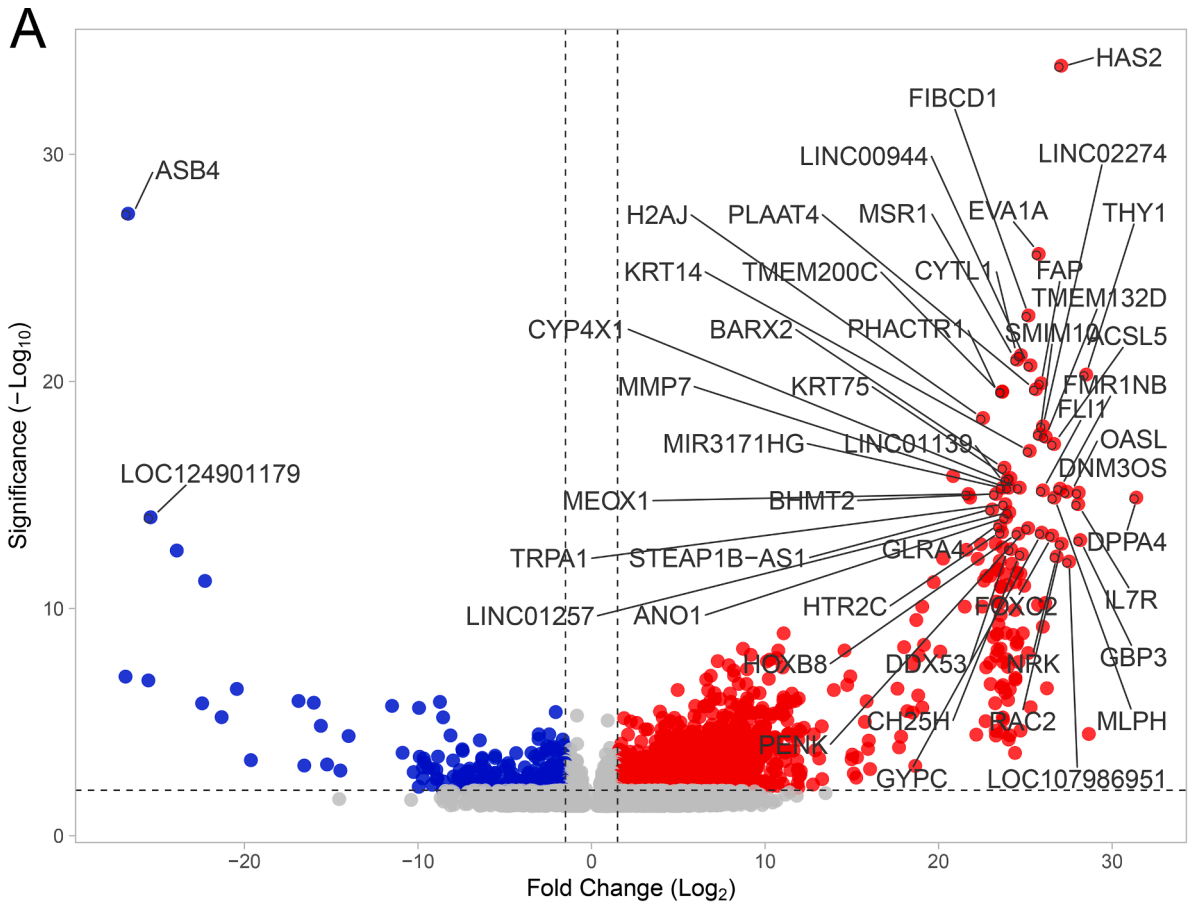

B

	Sensitive MB	Resistant MB
8h PVSRIPO	1029	814
24h PVSRIPO	1087	755
8h vs 24h PVSRIPO	328	141

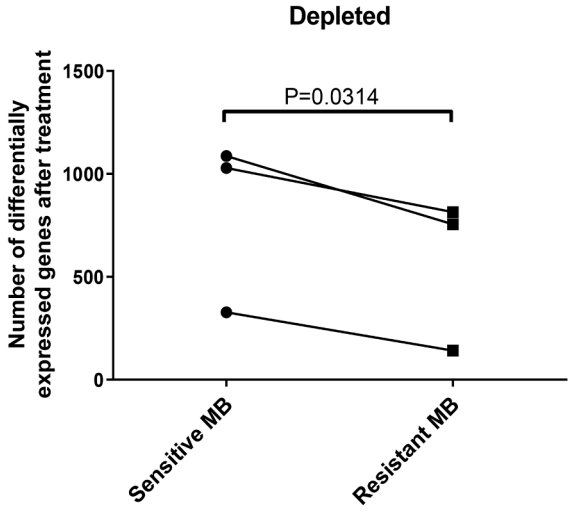

C

	Sensitive MB	Resistant MB
8h PVSRIPO	1453	899
24h PVSRIPO	1250	857
8h vs 24h PVSRIPO	78	121

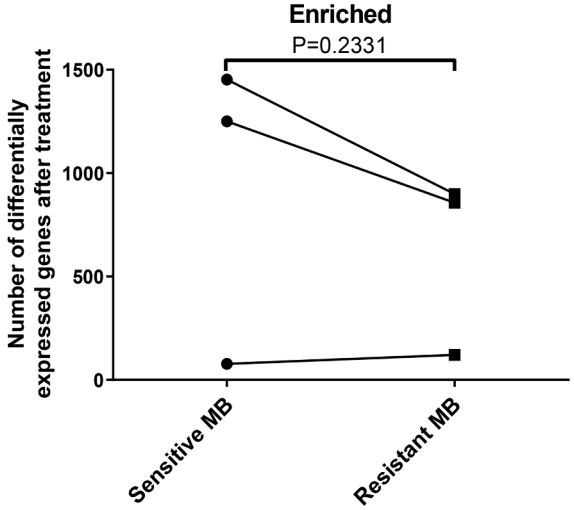

Fig. 5. Genetic activation is preferentially increased in "sensitive" medulloblastoma cell lines. (A) Volcano plot of untreated "resistant" medulloblastoma cells (D283 and D324) vs. "sensitive" (D341 and D556) cells demonstrates many more significantly more enriched differentially expressed cells in the sensitive group. (B) Line graphs demonstrating all significantly depleted genes in sensitive vs. resistance medulloblastoma cells. There were significantly more gene depletions in sensitive cells. (C) Line graphs demonstrating all significantly enriched genes in sensitive vs. resistant medulloblastoma cells with a trend toward more genes in the sensitive group.

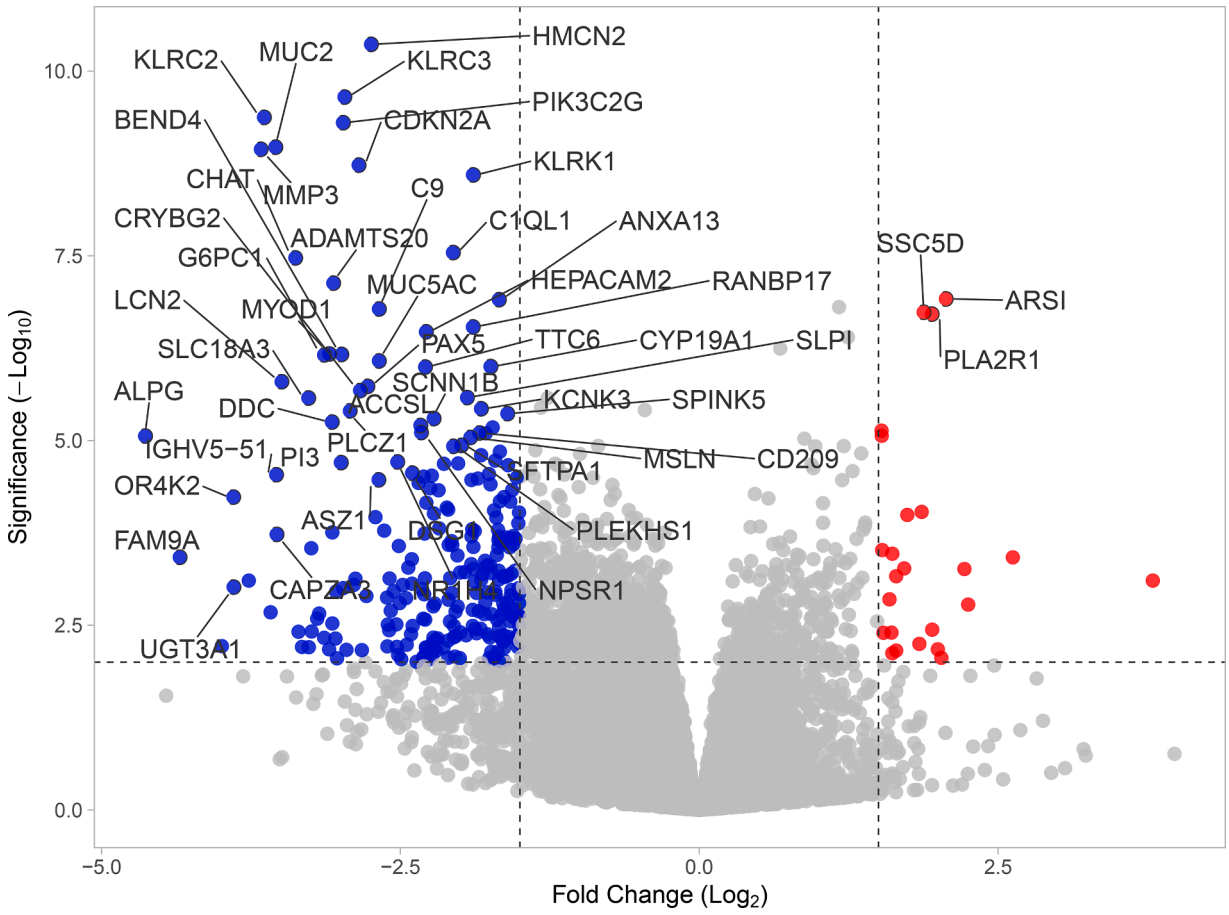

Fig. 6. Volcano plot of top 50 differentially expressed genes in $<$ and $\geq$ 1 year survival glioblastoma patient samples. Genes in blue are depleted in patients living $<$ 1 year ($N = 28$). Genes in red are enriched in patients living $\geq$ 1 year ($N = 29$).

recombinant, PVSRIPO, a single positive-strand RNA virus. Of the 32,117 genes analyzed, only five were found to be significantly shared by both: *GCLM, LANCL2,* and *RBM3* were enriched while *ADAMTS1 and VEGFA* were depleted. Table 1 contains a brief description of their function, however, there are no obvious commonalities amongst these genes. Notably, there is an increasing body of literature describing interactions of VEGF and viral immunotherapy; combining anti-VEGF treatment with virus increases outcomes in mice models compared to either alone [35–37]. Notably, *GCLM, LANCL2* were also significantly shared between pHGG and medulloblastoma cell treated with G207. Glutamate-cysteine ligase modifier subunit (GCLM) is the first rate limiting enzyme in glutathione synthesis while LanC-like protein 2 (LANCL2) is a negative transcription regulator. To our knowledge, there are no therapeutics that specifically target GCLM or LANCL2 thereby making the assessment of these entities challenging to assess if modulation can result in improved viral replication and lysis throughout a tumor.

Using data from a Phase II trial of PVSRIPO for recurrent adult glioblastoma, we highlighted genes that were both enriched or depleted in patients surviving greater than one year compared to less than 1 year. Notably, enrichment of the HALLMARK_EPITHELIAL_MESENCHYMAL_TRANSITION was associated with poor survival. This is somewhat expected given the 200 genes are associated with the epithelial mesenchymal transition in cancer, suggestive of more aggressive tumors that are likely less responsive to viral immunotherapy [30]. Additionally, we found the following genes in both PVSRIPO "resistant" medulloblastoma and "low" survival after treatment with PVSRIPO: *CCDC13, LGR6, LMO2, LUM, RARB, ADAMTS20, ANGPTL4, BEND, CSF1, FUT11, PCSK6, PLIN2,* and *PLS1*. It is noteworthy that colony stimulating factor 1 (*CSF1*), a cytokine controlling macrophage function, was depleted in these cohorts. Our group has found that higher myeloid cell density was associated with lower tumor mutational burden which was associated with longer survival after PVSRIPO administration [38]. Further work will determine if low CSF1 could be a clinical biomarker predicting poor response to viral immunotherapy.

In the context of Phase I clinical trials exploring PVSRIPO and G207 to treat malignant pediatric brain tumors, it is noteworthy that in both trials, only patients with recurrent pediatric high grade gliomas were enrolled [4,6]. Therefore, it is unknown if clinical responses and overall survival would differ in patients with newly diagnosed pHGG. In recurrent HGG, T cells are enriched in the perivascular region and immunosuppressive regulatory T cells are decreased [39]. Additionally, recurrent HGG have more tumor-infiltrating lymphocytes, macrophages, and PD-1 positive cells [40]. However, patients have profoundly decreased lymphocyte counts after chemoradiation. In a manuscript which analyzed data from four different clinical studies, lymphocyte counts were normal in 83% of patient before treatment compared to only 43% after chemoradiotherapy [41]. While some tumor characteristics may enhance immunotherapy at recurrence, profound systemic lymphopenia may severely limit the ability for the systemic immune system to respond. Additional studies of G207 and PVSRIPO to treat patients in the newly diagnosed setting are needed to resolve this uncertainty.

Limitations to our findings are as follow: 1) experiments using cell lines may have limited translational applicability, 2) "low" survival does not account for the multitude of other possible predictors of outcomes in glioblastoma clinical trials, and 3) the intrinsic limitations analyzing medulloblastoma cell line data with clinical data from an adult

Table 3
Differentially expressed genes shared by "low survival" glioblastoma and "resistant" medulloblastoma.

Genes: enriched	Full name	Function	Reference
CCDC13	coiled-coil domain containing 13	DNA damage response; microtubule and cilium organization	https://www.ncbi.nlm.nih.gov/gene/152206
LGR6	leucine rich repeat containing G protein-coupled receptor 6	G coupled protein hormone receptor	
LMO2	LIM domain only 2	Role in hematopoietic development	https://www.ncbi.nlm.nih.gov/gene/4005
LUM	lumican	Member of small leucine-rich proteoglycan family, regulates spacings in collagen	https://www.ncbi.nlm.nih.gov/gene/4060
RARB	retinoic acid receptor beta	Mediates embryonic morphogenesis, cell differentiation/growth	https://www.ncbi.nlm.nih.gov/gene/5915
Genes: depleted			
ADAMTS20	ADAM metallopeptidase with thrombospondin type 1 motif 20	Possibly involved in tissue remodeling	https://www.ncbi.nlm.nih.gov/gene/80070
ANGPTL4	angiopoietin like 4	Serum hormone regulating insulin sensitivity, lipid metabolism, glucose homeostasis; endothelial cell apoptosis survival factor	https://www.ncbi.nlm.nih.gov/gene/51129
BEND4	BEN domain containing 4	Possibly involved in DNA binding	https://www.ncbi.nlm.nih.gov/gene/389206
CSF1	colony stimulating factor 1	Cytokine involved in macrophage function and differentiation	https://www.ncbi.nlm.nih.gov/gene/1435
FUT11	fucosyltransferase 11	Possibly involved in fucosylation	https://www.ncbi.nlm.nih.gov/gene/170384
PCSK6	proprotein convertase subtilisin/kexin type 6	Processes peptide precursors in the secretory pathway	https://www.ncbi.nlm.nih.gov/gene/5046
PLIN2	perilipin 2	Coat lipid storage droplets intracellularly	https://www.ncbi.nlm.nih.gov/gene/123
PLS1	plastin 1	Actin binding proteins in most tissues	https://www.ncbi.nlm.nih.gov/gene/5357

glioblastoma clinical trial. However, the finding of these overlapping genes in different tumor types in both *in vitro* and clinic setting is also a strength that may indicate these genes are putative mediators of resistance to PVSRIPO. Furthermore, although the Phase 1b clinical trial of PVSRIPO for pediatric malignant brain tumors (NCT03043391) was open to patients with medulloblastoma as well as pHGG, only patients with pHGG were enrolled [4]. Therefore, no clinical data analyzing medulloblastoma cellular response to PVSRIPO was available to compare/contrast to the *in vitro* data in this work. Notably, the ongoing trial of G207 for pediatric cerebellar tumors (NCT03911388) is enrolling patients with medulloblastoma [29] and may provide additional insight into the findings of medulloblastoma cell lines treated with G207 in this work. Together, this work provides basic foundational data as to the mechanism of viral immunotherapy in pHGG and medulloblastoma and serves as the starting point to explore identified genes in further detail in order to optimize G207 and PVSRIPO for the treatment of malignant brain tumors.

CRediT authorship contribution statement

Eric M. Thompson: Conceptualization, Data curation, Formal analysis, Funding acquisition, Investigation, Methodology, Project administration, Resources, Supervision, Validation, Writing – original draft, Writing – review & editing. **Kyung-Don Kang:** Data curation, Formal analysis, Investigation, Methodology, Writing – review & editing. **Kevin Stevenson:** Data curation, Formal analysis, Investigation, Methodology, Software, Validation, Writing – review & editing. **Hengshan Zhang:** Data curation, Investigation, Methodology, Validation, Writing – review & editing. **Matthias Gromeier:** Resources, Writing – review & editing. **David Ashley:** Resources, Writing – review & editing. **Michael Brown:** Data curation, Methodology, Resources, Validation, Writing – review & editing. **Gregory K. Friedman:** Conceptualization, Data curation, Formal analysis, Funding acquisition, Investigation, Methodology, Project administration, Resources, Supervision, Validation, Writing – review & editing.

Declaration of competing interest

Two authors, Michael Brown and Matthias Gromeier own intellectual property related to PVSRIPO, which has been licensed to Istari Oncology, Inc. Matthias Gromeier holds equity in Istari Oncology, Inc. Drs. Brown and Gromeier received consultancy fees from Istari Oncology, Inc.

Data availability

RNA sequencing data from G207 and PVSRIPO treated cell lines is available at GSE233949. Other data will be considered by the authors on a case-by-case basis under a material transfer agreement.

Acknowledgments

Funding: American Brain Tumor Association, The Cure Starts Now, Department of Defense (CA171067), The Musella Foundation, Chetna and Meena Trust (EMT). Rally Foundation for Childhood Cancer Research, CureSearch for Children's Cancer, The V Foundation for Cancer Research, Andrew McDonough B+ Foundation, National Pediatric Cancer Foundation, and Pediatric Cancer Research Foundation (GKF). NIH P30 AR048311 and NIH P30 AI27667 grants (UAB Comprehensive Flow Cytometry Core Facility).

Supplementary materials

Supplementary material associated with this article can be found, in the online version, at doi:10.1016/j.tranon.2024.101875.

References

[1] A.M. Martin, E. Raabe, C. Eberhart, K.J. Cohen, Management of pediatric and adult patients with medulloblastoma, Curr. Treat. Options Oncol. 15 (2014) 581–594, https://doi.org/10.1007/s11864-014-0306-4.

[2] E.M. Thompson, T. Hielscher, E. Bouffet, M. Remke, B. Luu, S. Gururangan, R. E. McLendon, D.D. Bigner, E.S. Lipp, S. Perreault, Y.J. Cho, et al., Prognostic value of medulloblastoma extent of resection after accounting for molecular subgroup: a retrospective integrated clinical and molecular analysis, Lancet Oncol. 17 (2016) 484–495, https://doi.org/10.1016/S1470-2045(15)00581-1.

[3] R.I. Jakacki, K.J. Cohen, A. Buxton, M.D. Krailo, P.C. Burger, M.K. Rosenblum, D. J. Brat, R.L. Hamilton, S.P. Eckel, T. Zhou, R.S. Lavey, et al., Phase 2 study of concurrent radiotherapy and temozolomide followed by temozolomide and lomustine in the treatment of children with high-grade glioma: a report of the children's oncology group ACNS0423 study, Neuro. Oncol. 18 (2016) 1442–1450, https://doi.org/10.1093/neuonc/now038.

[4] E.M. Thompson, D. Landi, M.C. Brown, H.S. Friedman, R. McLendon, J. E. Herndon 2nd, E. Buckley, D.P. Bolognesi, E. Lipp, K. Schroeder, O.J. Becher, et al., Recombinant polio-rhinovirus immunotherapy for recurrent paediatric high-grade glioma: a phase 1b trial, Lancet Child Adolesc. Health (2023), https://doi.org/10.1016/S2352-4642(23)00031-7.

[5] A. Desjardins, M. Gromeier, J.E. Herndon 2nd, N. Beaubier, D.P. Bolognesi, A. H. Friedman, H.S. Friedman, F. McSherry, A.M. Muscat, S. Nair, K.B. Peters, et al., Recurrent glioblastoma treated with recombinant poliovirus, N. Engl. J. Med. 379 (2018) 150–161, https://doi.org/10.1056/NEJMoa1716435.

[6] G.K. Friedman, J.M. Johnston, A.K. Bag, J.D. Bernstock, R. Li, I. Aban, K. Kachurak, L. Nan, K.D. Kang, S. Totsch, C. Schlappi, et al., Oncolytic HSV-1 G207 immunovirotherapy for pediatric high-grade gliomas, N. Engl. J. Med. 384 (2021) 1613–1622, https://doi.org/10.1056/NEJMoa2024947.

[7] J.M. Markert, M.D. Medlock, S.D. Rabkin, G.Y. Gillespie, T. Todo, W.D. Hunter, C. A. Palmer, F. Feigenbaum, C. Tornatore, F. Tufaro, R.L. Martuza, Conditionally replicating herpes simplex virus mutant, G207 for the treatment of malignant glioma: results of a phase I trial, Gene Ther. 7 (2000) 867–874, https://doi.org/10.1038/sj.gt.3301205.

[8] J.M. Markert, S.N. Razdan, H.C. Kuo, A. Cantor, A. Knoll, M. Karrasch, L.B. Nabors, M. Markiewicz, B.S. Agee, J.M. Coleman, A.D. Lakeman, et al., A phase 1 trial of oncolytic HSV-1, G207, given in combination with radiation for recurrent GBM demonstrates safety and radiographic responses, Mol. Ther. 22 (2014) 1048–1055, https://doi.org/10.1038/mt.2014.22.

[9] J.M. Markert, P.G. Liechty, W. Wang, S. Gaston, E. Braz, M. Karrasch, L.B. Nabors, M. Markiewicz, A.D. Lakeman, C.A. Palmer, J.N. Parker, et al., Phase Ib trial of mutant herpes simplex virus G207 inoculated pre-and post-tumor resection for recurrent GBM, Mol. Ther. 17 (2009) 199–207, https://doi.org/10.1038/mt.2008.228.

[10] P.F. Jacobsen, D.J. Jenkyn, J.M. Papadimitriou, Establishment of a human medulloblastoma cell line and its heterotransplantation into nude mice, J. Neuropathol. Exp. Neurol. 44 (1985) 472–485, https://doi.org/10.1097/00005072-198509000-00003.

[11] H.S. Friedman, P.C. Burger, S.H. Bigner, J.Q. Trojanowski, C.J. Wikstrand, E. C. Halperin, D.D. Bigner, Establishment and characterization of the human medulloblastoma cell line and transplantable xenograft D283 Med, J. Neuropathol. Exp. Neurol. 44 (1985) 592–605, https://doi.org/10.1097/00005072-198511000-00005.

[12] H.S. Friedman, O.M. Colvin, S.X. Skapek, S.M. Ludeman, G.B. Elion, S.C. Schold Jr., P.F. Jacobsen, L.H. Muhlbaier, D.D Bigner, Experimental chemotherapy of human medulloblastoma cell lines and transplantable xenografts with bifunctional alkylating agents, Cancer Res. 48 (1988) 4189–4195.

[13] N. Aldosari, R.N. Wiltshire, A. Dutra, E. Schrock, R.E. McLendon, H.S. Friedman, D. D. Bigner, S.H. Bigner, Comprehensive molecular cytogenetic investigation of chromosomal abnormalities in human medulloblastoma cell lines and xenograft, Neuro. Oncol. 4 (2002) 75–85, https://doi.org/10.1093/neuonc/4.2.75.

[14] X.M. He, L.E. Ostrowski, M.A. von Wronski, H.S. Friedman, C.J. Wikstrand, S. H. Bigner, A. Rasheed, S.K. Batra, S. Mitra, T.P. Brent, et al., Expression of O6-methylguanine-DNA methyltransferase in six human medulloblastoma cell lines, Cancer Res. 52 (1992) 1144–1148.

[15] D.P. Ivanov, B. Coyle, D.A. Walker, A.M. Grabowska, *In vitro* models of medulloblastoma: choosing the right tool for the job, J. Biotechnol. 236 (2016) 10–25, https://doi.org/10.1016/j.jbiotec.2016.07.028.

[16] E.M. Thompson, S.T. Keir, T. Venkatraman, C. Lascola, K.W. Yeom, A.B. Nixon, Y. Liu, D. Picard, M. Remke, D.D. Bigner, V. Ramaswamy, et al., The role of angiogenesis in group 3 medulloblastoma pathogenesis and survival, Neuro. Oncol. 19 (2017) 1217–1227, https://doi.org/10.1093/neuonc/nox033.

[17] M.E. Dolan, A.E. Pegg, R.C. Moschel, B.R. Vishnuvajjala, K.P. Flora, M.R. Grever, H.S. Friedman, Biodistribution of O6-benzylguanine and its effectiveness against human brain tumor xenografts when given in polyethylene glycol or cremophor-EL, Cancer Chemother. Pharmacol. 35 (1994) 121–126, https://doi.org/10.1007/BF00686633.

[18] J. Ponten, E.H. Macintyre, Long term culture of normal and neoplastic human glia, Acta Pathol. Microbiol. Scand. 74 (1968) 465–486, https://doi.org/10.1111/j.1699-0463.1968.tb03502.x.

[19] M. Allen, M. Bjerke, H. Edlund, S. Nelander, B. Westermark, Origin of the U87MG glioma cell line: good news and bad news, Sci. Transl. Med. 8 (2016) 354re353, https://doi.org/10.1126/scitranslmed.aaf6853.

[20] G.K. Friedman, J.D. Bernstock, D. Chen, L. Nan, B.P. Moore, V.M. Kelly, S. L. Youngblood, C.P. Langford, X. Han, E.K. Ring, E.A. Beierle, et al., Enhanced sensitivity of patient-derived pediatric high-grade brain tumor xenografts to oncolytic HSV-1 virotherapy correlates with nectin-1 expression, Sci. Rep. 8 (2018) 13930, https://doi.org/10.1038/s41598-018-32353-x.

[21] M.C. Brown, E.K. Holl, D. Boczkowski, E. Dobrikova, M. Mosaheb, V. Chandramohan, D.D. Bigner, M. Gromeier, S.K. Nair, Cancer immunotherapy with recombinant poliovirus induces IFN-dominant activation of dendritic cells and tumor antigen-specific CTLs, Sci. Transl. Med. 9 (2017), https://doi.org/10.1126/scitranslmed.aan4220.

[22] E.M. Thompson, M. Brown, E. Dobrikova, V. Ramaswamy, M.D. Taylor, R. McLendon, J. Sanks, V. Chandramohan, D. Bigner, M. Gromeier, Poliovirus receptor (CD155) expression in pediatric brain tumors mediates oncolysis of medulloblastoma and pleomorphic xanthoastrocytoma, J. Neuropathol. Exp. Neurol. 77 (2018) 696–702, https://doi.org/10.1093/jnen/nly045.

[23] M.C. Brown, J.D. Bryant, E.Y. Dobrikova, M. Shveygert, S.S. Bradrick, V. Chandramohan, D.D. Bigner, M. Gromeier, Induction of viral, 7-methyl-guanosine cap-independent translation and oncolysis by mitogen-activated protein kinase-interacting kinase-mediated effects on the serine/arginine-rich protein kinase, J. Virol. 88 (2014) 13135–13148, https://doi.org/10.1128/JVI.01883-14.

[24] A.C. Shah, K.H. Price, J.N. Parker, S.L. Samuel, S. Meleth, K.A. Cassady, G. Y. Gillespie, R.J. Whitley, J.M. Markert, Serial passage through human glioma xenografts selects for a deltagamma134.5 herpes simplex virus type 1 mutant that exhibits decreased neurotoxicity and prolongs survival of mice with experimental brain tumors, J. Virol. 80 (2006) 7308–7315, https://doi.org/10.1128/JVI.00725-06.

[25] J.K. Jones, H. Zhang, A.M. Lyne, F.M.G. Cavalli, W.E. Hassen, K. Stevenson, R. Kornahrens, Y. Yang, S. Li, S. Dell, Z.J. Reitman, et al., ABL1 and ABL2 promote medulloblastoma leptomeningeal dissemination, Neurooncol. Adv. 5 (2023) vdad095, https://doi.org/10.1093/noajnl/vdad095.

[26] J. Goedhart, M.S. Luijsterburg, VolcaNoseR is a web app for creating, exploring, labeling and sharing volcano plots, Sci. Rep. 10 (2020) 20560, https://doi.org/10.1038/s41598-020-76603-3.

[27] V. Chandramohan, J.D. Bryant, H. Piao, S.T. Keir, E.S. Lipp, M. Lefaivre, K. Perkinson, D.D. Bigner, M. Gromeier, R.E. McLendon, Validation of an immunohistochemistry assay for detection of CD155, the poliovirus receptor, in malignant gliomas, Arch. Pathol. Lab. Med. 141 (2017) 1697–1704, https://doi.org/10.5858/arpa.2016-0580-OA.

[28] A. Liberzon, C. Birger, H. Thorvaldsdottir, M. Ghandi, J.P. Mesirov, P. Tamayo, The molecular signatures database (MSigDB) hallmark gene set collection, Cell Syst. 1 (2015) 417–425, https://doi.org/10.1016/j.cels.2015.12.004.

[29] J.D. Bernstock, A.K. Bag, J. Fiveash, K. Kachurak, G. Elsayed, G. Chagoya, F. Gessler, P.A. Valdes, A. Madan-Swain, R. Whitley, J.M. Markert, et al., Design and rationale for first-in-human phase 1 immunovirotherapy clinical trial of oncolytic HSV G207 to treat malignant pediatric cerebellar brain tumors, Hum. Gene Ther. 31 (2020) 1132–1139, https://doi.org/10.1089/hum.2020.101.

[30] R. Kalluri, R.A. Weinberg, The basics of epithelial-mesenchymal transition, J. Clin. Invest. 119 (2009) 1420–1428, https://doi.org/10.1172/JCI39104.

[31] M.C. Brown, M.M. Mosaheb, M. Mohme, Z.P. McKay, E.K. Holl, J.P. Kastan, Y. Yang, G.M. Beasley, E.S. Hwang, D.M. Ashley, D.D. Bigner, et al., Viral infection of cells within the tumor microenvironment mediates antitumor immunotherapy via selective TBK1-IRF3 signaling, Nat. Commun. 12 (2021) 1858, https://doi.org/10.1038/s41467-021-22088-1.

[32] Y. Yang, M.C. Brown, G. Zhang, K. Stevenson, M. Mohme, R. Kornahrens, D. D. Bigner, D.M. Ashley, G.Y. Lopez, M. Gromeier, Polio virotherapy targets the malignant glioma myeloid infiltrate with diffuse microglia activation engulfing the CNS, Neuro. Oncol. (2023), https://doi.org/10.1093/neuonc/noad052.

[33] M.M. Mosaheb, E.Y. Dobrikova, M.C. Brown, Y. Yang, J. Cable, H. Okada, S.K. Nair, D.D. Bigner, D.M. Ashley, M. Gromeier, Genetically stable poliovirus vectors activate dendritic cells and prime antitumor CD8 T cell immunity, Nat. Commun. 11 (2020) 524, https://doi.org/10.1038/s41467-019-13939-z.

[34] D. Saha, R.L. Martuza, S.D. Rabkin, Macrophage polarization contributes to glioblastoma eradication by combination immunovirotherapy and immune checkpoint blockade, Cancer Cell 32 (2017) 253–267, https://doi.org/10.1016/j.ccell.2017.07.006, e255.

[35] J.Y. Wang, The capable ABL: what is its biological function? Mol. Cell. Biol. 34 (2014) 1188–1197, https://doi.org/10.1128/MCB.01454-13.

[36] F.K. Eshun, M.A. Currier, R.A. Gillespie, J.L. Fitzpatrick, W.H. Baird, T.P. Cripe, VEGF blockade decreases the tumor uptake of systemic oncolytic herpes virus but enhances therapeutic efficacy when given after virotherapy, Gene Ther. 17 (2010) 922–929, https://doi.org/10.1038/gt.2010.82.

[37] T. Kottke, G. Hall, J. Pulido, R.M. Diaz, J. Thompson, H. Chong, P. Selby, M. Coffey, H. Pandha, J. Chester, A. Melcher, et al., Antiangiogenic cancer therapy combined with oncolytic virotherapy leads to regression of established tumors in mice, J. Clin. Invest. 120 (2010) 1551–1560, https://doi.org/10.1172/JCI41431.

[38] M. Gromeier, M.C. Brown, G. Zhang, X. Lin, Y. Chen, Z. Wei, N. Beaubier, H. Yan, Y. He, A. Desjardins, J.E. Herndon 2nd, et al., Very low mutation burden is a

feature of inflamed recurrent glioblastomas responsive to cancer immunotherapy, Nat. Commun. 12 (2021) 352, https://doi.org/10.1038/s41467-020-20469-6.
[39] C. Alanio, Z.A. Binder, R.B. Chang, M.P. Nasrallah, D. Delman, J.H. Li, O.Y. Tang, L.Y. Zhang, J.V. Zhang, E.J. Wherry, D.M. O'Rourke, et al., Immunologic features in de novo and recurrent glioblastoma are associated with survival outcomes, Cancer Immunol. Res. 10 (2022) 800–810, https://doi.org/10.1158/2326-6066.CIR-21-1050.
[40] F. Wang, S.J. Cathcart, D.J. DiMaio, N. Zhao, J. Chen, M.R. Aizenberg, N. A. Shonka, C. Lin, C. Zhang, Comparison of tumor immune environment between newly diagnosed and recurrent glioblastoma including matched patients, J. Neurooncol. 159 (2022) 163–175, https://doi.org/10.1007/s11060-022-04053-0.
[41] S.A. Grossman, S. Ellsworth, J. Campian, A.T. Wild, J.M. Herman, D. Laheru, M. Brock, A. Balmanoukian, X Ye, Survival in patients with severe lymphopenia following treatment with radiation and chemotherapy for newly diagnosed solid tumors, J. Natl. Compr. Canc. Netw. 13 (2015) 1225–1231, https://doi.org/10.6004/jnccn.2015.0151.